Cost-Effective 40-Gbaud THP PS-PAM-4 C-Band IM/DD Transmission for 50-km Inter-DCI Utilizing 2-bit DAC

Zhuo Chen, Zipeng Liang, Junyu Wu, Weiqi Lu, Xinyu Chang, Xiaoxiao Dai, *Member, IEEE*, Qi Yang, Chen Liu, Mengfan Cheng, *Senior Member, IEEE*, Lei Deng, Deming Liu, and William Shieh, *Fellow, IEEE*

***Abstract*—Data center interconnections are cost-sensitive. We propose and demonstrate a cost-effective C-band intensity modulation direct detection (IM/DD) transmitter for extended range (ER) inter-datacenter interconnects utilizing only a 2-bit digital-to-analog converter (DAC). Tomlinson-Harashima precoding (THP) is used in transmitter DSP to compensate for dispersion-induced impairments. Due to the uniform distribution of signal levels after THP encoding, a high-resolution DAC is required to generate electrical signals. The hardware cost of the transmitter can be significantly reduced by compressing the physical number of bits (PNOB) of the DAC to 2 bits. We quantize the signal to 4 levels and utilize up-sampling and noise shaping to greatly reduce the in-band quantization noise. The in-band signal to noise ratio (SNR) can be increased to 23 dB. We experimentally demonstrate a cost-effective 40-Gbaud probabilistic shaping PAM-4 C-band IM/DD transmission over 50-km utilizing only a 2-bit DAC in the transmitter without any optical dispersion compensation. The performance of the proposed scheme is proximate to the common case of using an 8-bit DAC. It has a BER gap of about 2×10^{-3} only when the received optical power (ROP) is higher than -6 dBm.**

***Index Terms*—Data center interconnection, digital-to-analog converter, tomlinson-harashima precoding, intensity modulation direct detection.**

I. Introduction

THE growing capacity demand for cloud-computing and Internet of Things has led to a swift increase in the requirement for transmission capacity for inter-datacenter interconnects (inter-DCI) [1]. Edge data centers require several tens of kilometers of optical fibers for interconnection. Due to the sensitivity of data center scenarios to cost and power consumption, there is significant interest in utilizing intensity modulation direct detection (IM/DD) schemes to achieve 100 Gb/s/λ extended range (ER) Ethernet connectivity. To address system bandwidth limitations, DSP is required at the transmitter side of 100G IM/DD systems to compress signal bandwidth. Techniques such as root raised cosine (RRC) filtering and pre-emphasis are typically used to achieve this. Furthermore, for standard single mode fiber (SSMF), the attenuation in C-band is much lower than that in O-band, which can support longer distance transmissions and higher power budget. The major limitation of the reach and capacity of C-band IM/DD transmission lies in the dispersion induced power fading effect, which is hard to be compensated using common linear equalizers. To extend the transmission range beyond 40 km, the use of digital dispersion compensation instead of optical methods can also significantly reduce the cost. One solution is Tomlinson-Harashima precoding (THP), which can extend the reach of 42-Gbaud C-band PAM-4 transmission to over 80 km [2], [3]. The processed PAM-4 signal is no longer 4-level signal, which must be generated by a high-resolution ($\geq$8) DAC. Reducing the resolution of the DAC can further compress the cost and power consumption [4]. Using the Gerchberg-Saxton algorithm and noise shaping, a 56-Gb/s PAM-4 signal for 80-km SSMF transmission in C-band is experimentally demonstrated utilizing a 4-bit DAC [5], [6]. A 32-Gbaud IM/DD PAM-4 signal is transmitted over 10-km SSMF using a 3-bit DAC and error-feedback noise shaping [7]. To further increase the transmission rate as well as to reduce the cost of the transmitter, using high-speed 2-bit ports instead of DACs is necessary. Commercial implementation of Gerchberg-Saxton algorithms and digital resolution enhancer at high sampling rates is difficult. Combining THP algorithm with simple quantization noise shaping is a promising candidate for the 400-GbE long-haul distance data center interconnects.

400Gb/s Ethernet and next-generation 800GbE require 224-Gb/s PAM-4 SerDes transceivers, which are almost close to commercialization [8], [9]. Therefore, we first compress the

Manuscript received 3 February 2024; revised 29 April 2024; accepted 9 May 2024. Date of publication 14 May 2024; date of current version 24 May 2024. This work was supported in part by the National Natural Science Foundation of China under Grant 62205115 and Grant 62275091 and in part by the National Key Research and Development Program of China under Grant 2021YFB1808200. *(Corresponding authors: Qi Yang; William Shieh.)*

Zhuo Chen, Zipeng Liang, Weiqi Lu, and Xinyu Chang are with the School of Optical and Electronic Information, Huazhong University of Science and Technology, Wuhan 430074, China (e-mail: chen_zhuo_@hust.edu.cn; liangzipeng@hust.edu.cn; luweiqi@hust.edu.cn; xinyu_chang@hust.edu.cn).

Junyu Wu and William Shieh are with the School of Engineering, Westlake University, Hangzhou 310010, China (e-mail: wujunyu@westlake.edu.cn; shiehw@westlake.edu.cn).

Xiaoxiao Dai, Qi Yang, Chen Liu, Mengfan Cheng, Lei Deng, and Deming Liu are with the School of Optical and Electronic Information, Huazhong University of Science and Technology, Wuhan 430074, China, and also with the Jinyinhu Laboratory, Wuhan 430040, China (e-mail: daixx@hust.edu.cn; yangqi@hust.edu.cn; liuchen@hust.edu.cn; chengmf@mail.hust.edu.cn; denglei_hust@mail.hust.edu.cn; dmliu@hust.edu.cn).

Digital Object Identifier 10.1109/JPHOT.2024.3400791

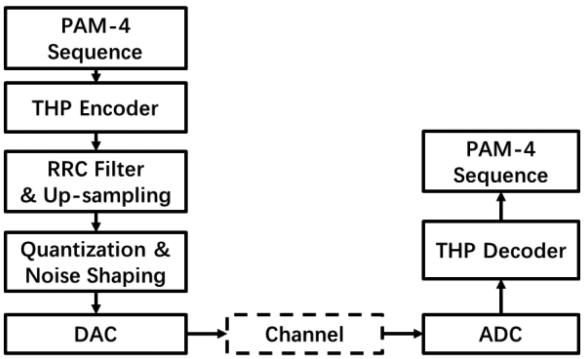

Fig. 1. Framework of the proposed scheme.

resolution of the DACs in transmitters for middle-range DCI with C-band IM/DD transmission to 2 bits. In implementation, the 2-bit signal can be generated by a PAM-4 SerDes transceiver, which is more cost-effective than the conventional transmitter using high-resolution DACs. The signal can also be built using inexpensive analog-multiplexers (AMUX), which interleaves the outputs of several low-speed PAM-4 IO ports in the time domain [10], [11]. The proposed scheme is much closer to commercialization than schemes using high-speed DACs. In the proposed scheme, THP has been used to compensate the dispersion damage of the signal. We apply up-sampling operation and noise shaping [12], [13] to quantize the signal to 4 levels and greatly reduce the in-band quantization noise. Weighing performance and complexity, a conventional pre-designed FIR filter is used for noise shaping in our scheme rather than a channel response-dependent FIR filter. The fixed FIR taps, which require no training, make hardware implementation simpler and more cost-effective. We experimentally transmit C-band 40-Gbaud probabilistic shaping (PS) PAM-4 signal in a 50-km SSMF transmission without any optical dispersion compensation. After 50-km SSMF transmission, the bit error rate (BER) performance is below the 15.3% overhead open forward error correction (OFEC) threshold.

II. Precoding and Noise Shaping

Fig. 1 illustrates the framework of the proposed scheme, encompassing quantization noise shaping and THP. THP serves to expand the transmission distance for a dispersion-limited IM/DD system. It consists of a feedback circuit and a $2M$ modulo operation. The transfer function of the feedback circuit has several poles which matches the zeros of the dispersion transfer function. It can be expressed as:

$$\frac{1}{1+H(z)} = \frac{1}{1+[R(z)-1]} = \frac{1}{R(z)} = R^{-1}(z) \quad (1)$$

where $H(z) = R(z) - 1$, and $R(z)$ is the dispersion-limited channel transfer function [14]. The modulo operation limits the amplitude-range of the coded signal within [-M, M). The coefficients of $H(z)$ can be obtained with an error-free decision-feedback equalizer (DFE) at the receiver side when transmitting un-coded PAM signal. As is shown in Fig. 2(a), THP encoding

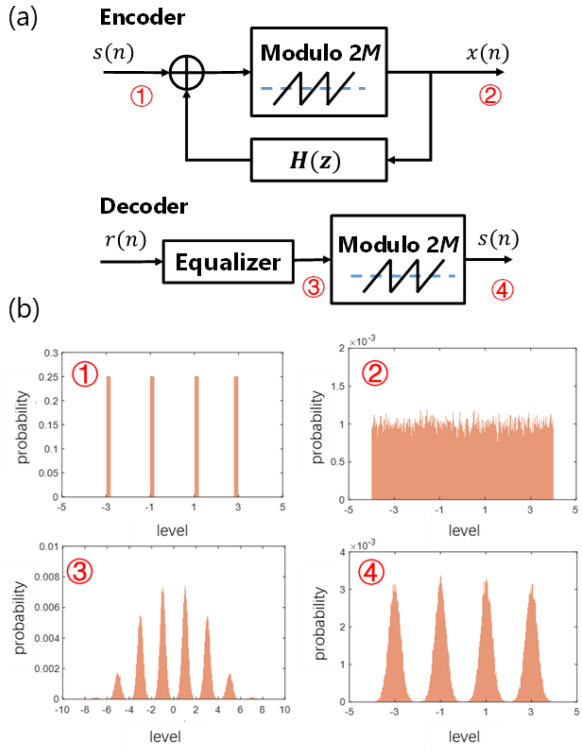

Fig. 2. (a) Structure of THP encoder and decoder; (b) waveform amplitude distributions at each node in the THP encoding/decoding process.

process can be expressed as:

$$x(n) = s(n) + a(n) + \sum_{i=1}^{l} h_i x(n-i) \quad (2)$$

where s and x are the original symbols and encoded signals. h are the coefficients of $H(z)$. $a \in 2M \cdot k$ (k is an integer) is introduced by modulo operation to limit the output signal level. a can be eliminated by modulo operation when decoding.

Since the THP replaces the feedback part of the DFE of the original receiver-side DSP, it only compensates the power fading induced by the dispersion. The feed-forward part of the DFE is not included in the THP. The remaining channel distortion, such as bandwidth limitation, still requires a feed-forward equalizer (FFE) to compensate at the receiver side. Therefore, the original PAM signal can be recovered by an FFE and modulo operation when decoding. Besides, to compensate the extra nonlinear distortion of the signal induced by MZM and fiber link, we replace the FFE by a 2-order polynomial nonlinear equalizer (PNLE), which can be expressed as:

$$y(n) = \sum_{k_1=-\lfloor (N_1-1)/2 \rfloor}^{\lfloor (N_1-1)/2 \rfloor} b_{1,k_1} x(n-k_1) + \sum_{k_2=-\lfloor (N_2-1)/2 \rfloor}^{\lfloor (N_2-1)/2 \rfloor} b_{2,k_2} x^2(n-k_2) \quad (3)$$

where b_{1,k_1} and b_{2,k_2} are the linear and nonlinear taps. $\lfloor \cdot \rfloor$ denotes the rounding down function. Using PNLE adds only $2 \cdot N_2$

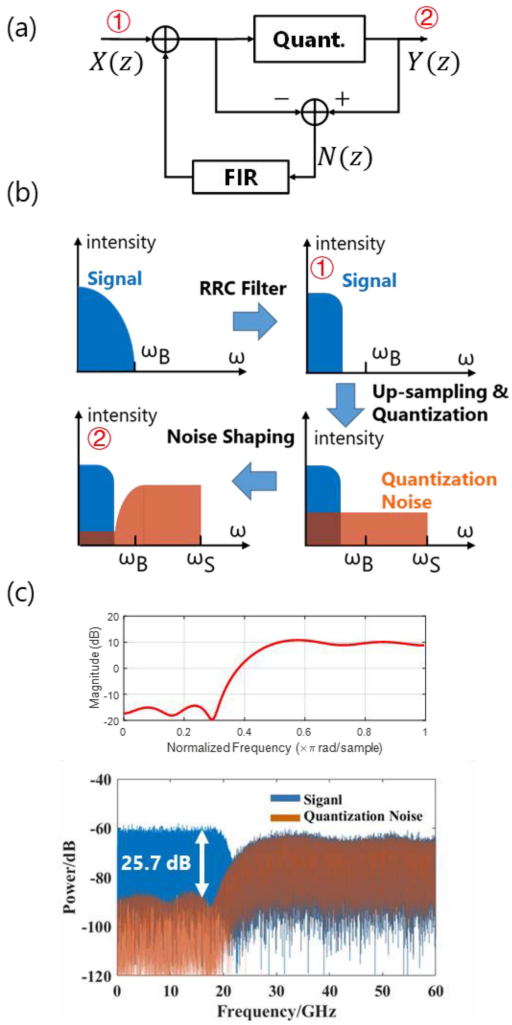

Fig. 3. (a) Structure of quantization noise shaping. (b) Principle of noise shaping in frequency-domain. (c) Frequency response of the FIR filter, the spectrums of the 2-bit output signal, and that of the quantization noise.

multipliers per symbol compared to FFE, which is affordable. The initial PNLE taps are obtained with training sequences, and then tracked with the decision directed least-mean square (DD-LMS) algorithm.

After THP, as is shown in Fig. 2(b)-②, the amplitude of the signal is distributed across the range of [- 4, 4] instead of being concentrated in four levels. The homogeneously distributed signal requires a high-resolution DAC to generate. Consequently, to transmit the signal utilizing 2-bit DAC, a simple noise shaping method is applied to compress the quantization noise. Fig. 3(a) shows the structure of noise shaping technique. As is shown in Fig. 3(b), a RRC filter is first applied on the signal after THP to compress the electrical bandwidth. Afterwards the signal is up-sampled from the Nyquist sampling rate to a higher sampling rate. Oversampling can spread the quantization noise over a larger range. Noise shaping transfers the energy of the quantization noise from the low-frequency end to the high-frequency end, which reduces the in-band noise substantially. Due to the high quantization noise caused by the use of a 2-bit DAC, up-sampling is necessary to make the SNR acceptable. The proposed scheme only requires an oversampling rate of 1.5. The 2-bit signal can be generated by high-speed PAM-4 SerDes transceiver in practical implementation. It can also be built using inexpensive AMUX with several low-speed IO ports. Using 8-bits resolution DAC chips over 60 GSa/s is much more expensive than several low-speed PAM-4 IO ports with AMUX. The frequency shape of the quantization noise depends on the response of the FIR filter in the feedback circuit. The process can be expressed as:

$$Y(z) = X(z) + (1 + F(z))N(z) \tag{4}$$

where X and Y are the input and output signals. N is the quantization noise. F is the FIR filter. The taps of FIR can be obtained by:

$$F = -\begin{bmatrix} A_r \\ A_i \end{bmatrix}^{-1} \begin{bmatrix} W \cdot \mathbf{1} \\ \mathbf{0} \end{bmatrix} \tag{5}$$

$$A(\omega) = W \begin{bmatrix} e^{-j\omega_1} & e^{-j2\omega_1} & \cdots & e^{-jn\omega_1} \\ e^{-j\omega_2} & e^{-j2\omega_2} & \cdots & e^{-jn\omega_2} \\ \vdots & \vdots & \ddots & \vdots \\ e^{-j\omega_s} & e^{-j2\omega_s} & \cdots & e^{-jn\omega_s} \end{bmatrix} \tag{6}$$

where $[\cdot]^{-1}$ denotes the Moore-Penrose pseudoinverse of a matrix. A_r and A_i are the real and imaginary parts of A. $\{\omega_1, \omega_2, \ldots, \omega_s\} = \{1, 2, \ldots, \mathrm{s}\}\ /\mathrm{s}\pi$ are uniformly-spaced frequencies of the signal. n is the number of FIR taps. $W = \mathrm{diag}(w,\ w \cdots w,\ 1,\ 1 \cdots 1)$. w is the weight that determines the stop-band attenuation. The numbers of w determines the stop-band width. ***1*** and ***0***are vectors of ones and zeros.

Fig. 3(c) shows the spectrums of the 2-bit signal and the shaped quantization noise, as well as the frequency response of the 9-tap FIR filter. It can be observed that most of the quantization noise is transferred out of the signal band. The spectrum of the noise is the same as the response shape of the FIR filter. The in-band signal to noise ratio is 25.7 dB, which is capable of supporting the IM/DD transmission.

III. Simulation and Discussion

In this section, in order to optimize the parameters in the scheme, we simulate a 40-km SSMF IM/DD transmission system. The DSP of transmitter and receiver is set as the Fig. 1 shows. The baud rate of PAM-4 sequence is set at 40 Gbaud. The sampling rate of 2-bit DAC is 120GSa/s. In the simulation, ignoring the nonlinear distortion of MZM and DACs, we use FFE in the THP decoding.

To balance between the computational complexity of THP and the performance of the system, we first analyze the relationship between the number of taps and the BER. Since the performance of THP is mainly related to the dispersion of the link, quantization noise shaping is not considered in this case. The signal after THP is generated by a 10-bit DAC. As is stated in Section II, THP essentially functions as a zero-error propagation DFE at the transmitter side. Its taps are obtained by training at the receiver side using error-free DFE. Fig. 4 shows the SNR versus the number of THP and error-free DFE feedback taps curves in the 40-km transmission. The number of the feedforward taps of the DFE and the FFE in THP decoding are both 51. The SNR

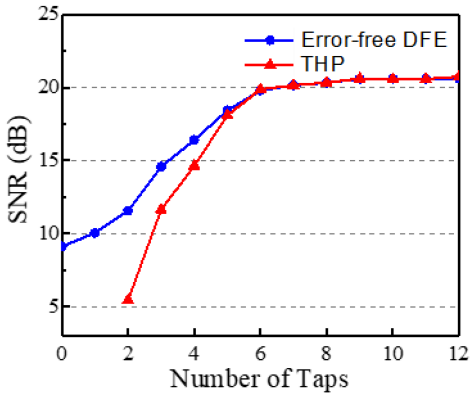

Fig. 4. SNR of the PAM-4 signal at the receiver end versus number of taps of the THP and error-free DFE in DSP for 40-km SSMF 40-Gbaud PAM-4 transmission.

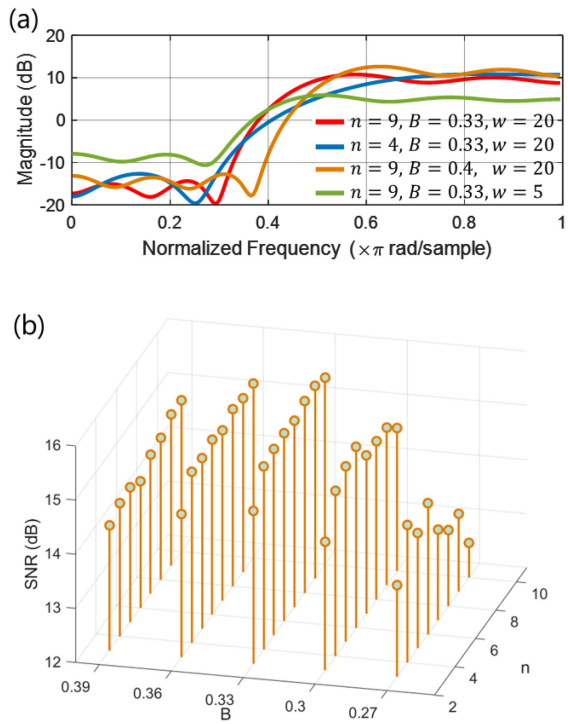

Fig. 5. (a) The frequency responses of the FIR filters generated using different parameters in the weight matrix; (b) SNR of the PAM-4 signal at receiver end versus taps number n and stopband width B for weight matrix W in FIR filter generation.

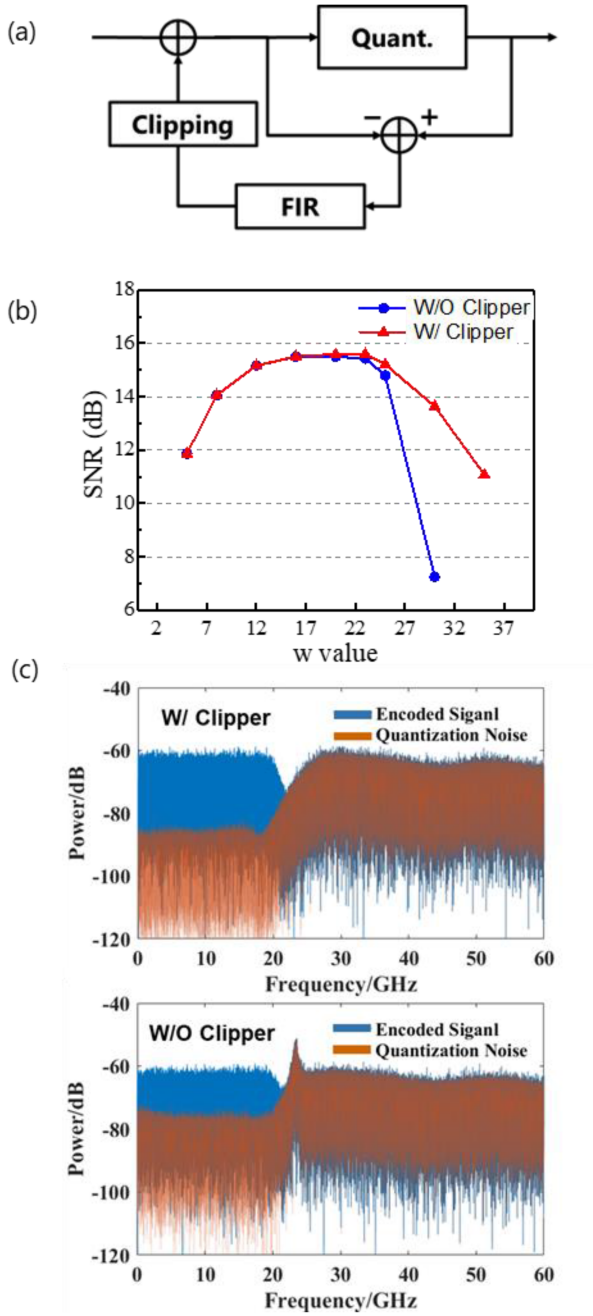

Fig. 6. (a) Structure of quantization noise shaping with additional noise clipper; (b) SNR versus w value of the weight matrix W for noise shaping with and without noise clipping; (c) the spectrums of the 2-bit output signal and the quantization noise using noise shaping with/without clipper ($w = 30$).

of the system increases when the number of feedback taps increases. Weighing the complexity and performance, the optimal number of feedback taps is 9 for 40-km transmission. Besides, at high SNRs, the performance of THP is close to using an error-free DFE at receiver end when the number of feedback taps is higher than 5. At low SNRs, the THP performance is impacted by modulo loss and is much lower than that of error-free DFE. Modulo operation may mistake the points at the boundary of $[-4, 4]$ for symbols at the opposite boundary [15]. Therefore, using probabilistic shaping PAM-4 modulation to reduce the probability of ± 3 symbols at the boundary can effectively reduce the modulo loss. In the experiment, probabilistic shaping is utilized to further extend the transmission reach.

The shape of quantization noise is determined by the FIR filter. The frequency response of the FIR filter is controlled by the weight matrix W, as shown in (5) and (6). The size of the diagonal matrix n is equal to the number of taps in the FIR filter. Fig. 5(a) shows the frequency responses of FIR filters with different parameters. Increasing the number of taps n results in a filter response that approaches a rectangular shape. The ratio of the number of weights $w$and 1 in the diagonal

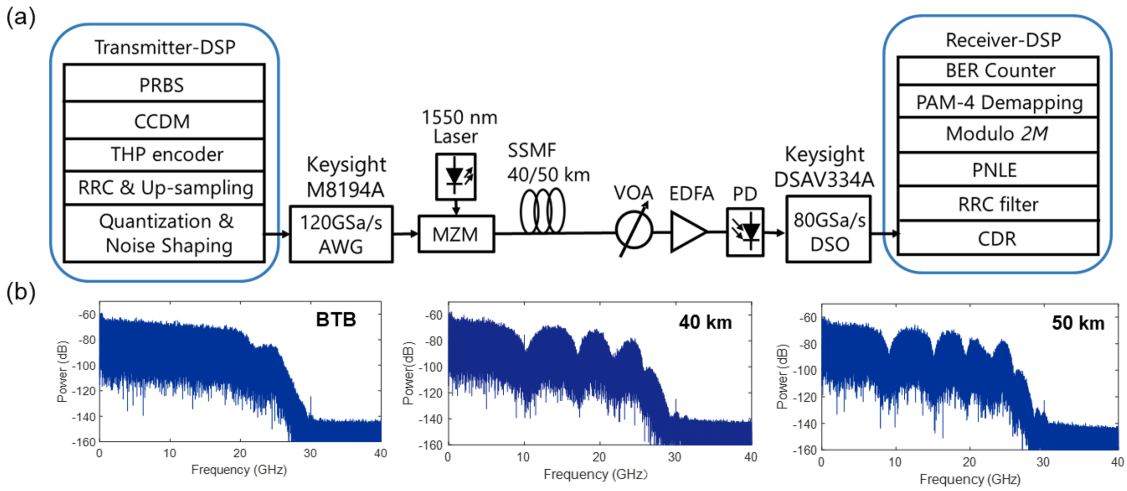

Fig. 7. (a) Experimental setup of the IM/DD transmission; (b) electrical spectrums of received signal at back-to-back and after 40/50-km transmission.

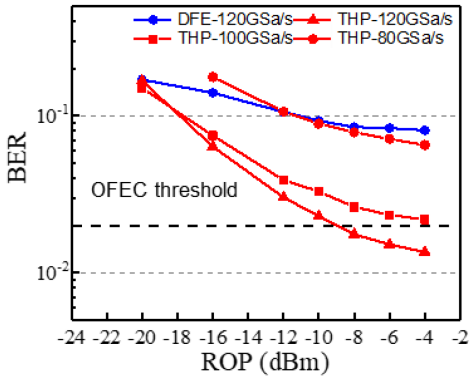

Fig. 8. BER versus ROP for 40-km 40-Gbaud PAM-4 transmission using THP/DFE and different up-sampling rate.

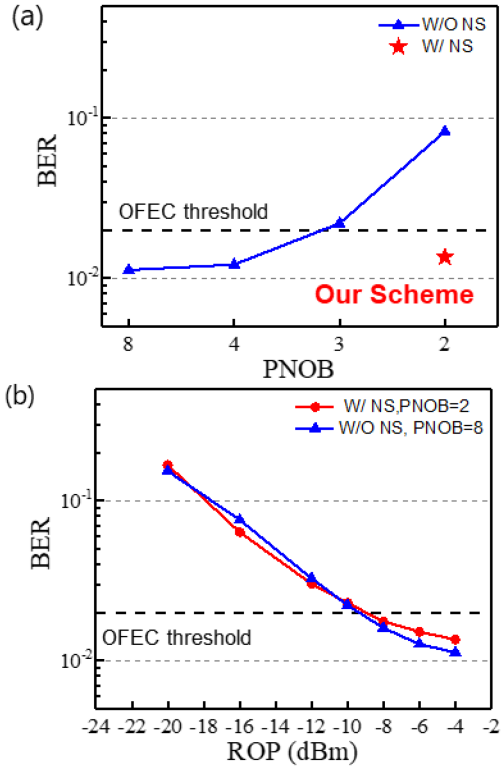

Fig. 9. (a) BER versus PNOB of DAC for 40-km transmissions with and without noise shaping at ROP of −4 dBm; (b) BER versus ROP for the proposed scheme and common case using 8-bit DAC.

matrix determines the filter's stopband width. It is defined as the normalized bandwidth B. We sweep the value of n and B to ensure the SNR at the receiver side is maximized. As is shown in Fig. 5(b), the optimal n and B values are 9 and 0.33, respectively.

A larger w value results in greater stopband attenuation, which pushes more quantization noise out of the signal band. However too large a value of w leads to excessive quantization noise feedback. The probability of noise spikes in the feedback circuit increases, making the feedback unstable. Also, as a result, the signal amplitude before the quantizer may exceed the quantization range [16]. Adding a clipper to the feedback circuit attenuates the effects of quantization noise spikes and stabilizes the feedback circuit, as is shown in Fig. 6(a). Nevertheless, the additional clipping noise will still degrade the SNR. The mathematical analysis of the system is complicated by the fact that both THP and noise shaping contain feedback loops. Therefore, we use simulation to determine the optimal w value. Fig. 6(b) shows the SNR versus w value of 40 Gbaud PAM-4 signal over 40-km SSMF transmission. The number of THP taps is 9, and the n and B of the weight matrix W are 9 and 0.33. With the w value increasing, the in-band SNR increases and BER performance improves. The performance reaches the peak at the w of 20. Fig. 6(c) reveals the function of the clipper added in the feedback circuit. It presents the frequency spectrums of the signal and quantization noise with and without clippers at the w of 30. The clippers ensure that the noise transfer model for the noise shaping remains valid. In the transmitter DSP, the THP encoder requires 9 multipliers per symbol. The noise shaping requires $3 \times 9 = 27$ multipliers per symbol. Up-sampling only changes sampling rate of noise shaping and increases the number of multipliers per symbol required from 18 to 27. The sampling rate of other DSPs

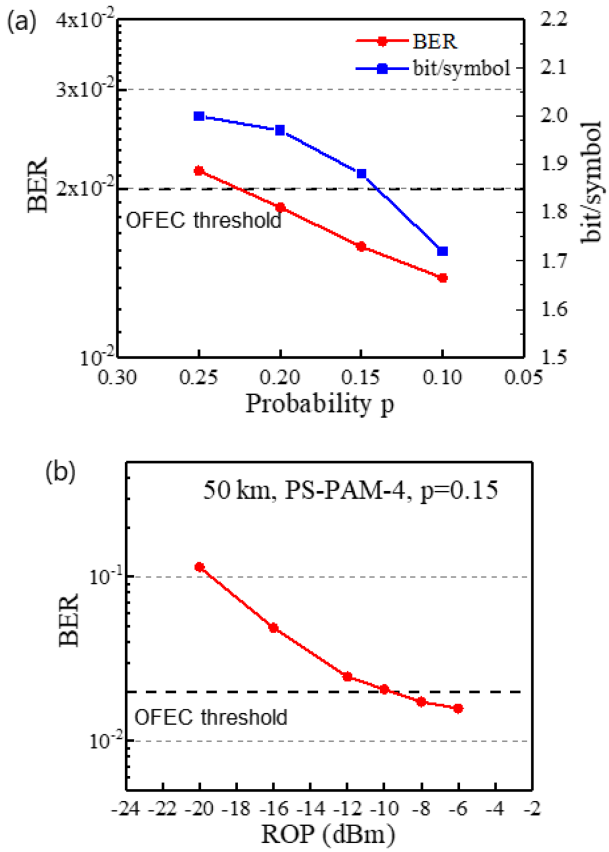

Fig. 10. (a) BER and bit-per-symbol rate versus the probability $\boldsymbol{p}$ curves; (b) BER versus ROP curve of PS-PAM-4 50-km transmission.

remain unchanged. The additional 9 multipliers only account for a very small percentage of the hardware resources required for the entire DSP of the transmitter. Although the noise shaping requires a higher clock rate for implementation, the additional cost and power consumption of the DSP chips for a less than 50% increase in clock rate is still much less than the savings achieved by using PAM-4 IO ports instead of 8-bit DACs. Meanwhile, up-sampling and noise shaping does not change the bandwidth of the original signal. The sampling rate required by the receiver will not be increased. The complexity of the DSP at receiver side is almost the same with traditional PAM-4 IM/DD systems.

IV. Experiment Setup

The experimental setup and DSP for the 40-Gbaud C-band IM/DD transmission system are shown in Fig. 7(a). In the transmitter side DSP, a binary sequence is first mapped into PAM-4 format with constant composition distribution matching (CCDM) for probabilistic shaping [17]. Afterwards THP with 9 feedback taps trained at receiver side using DFE is applied to the PAM-4 sequence. Then the 40-Gbaud PAM-4 sequence is up-sampled and reshaped by a RRC filter with roll-off factor of 0.1 to narrow the electrical bandwidth. Then the signal is quantized to 4 levels and applied with the quantization noise shaper. In this experiment, we use an arbitrary waveform generator (AWG, Keysight M8194A) to simulate a high-speed 2-bit DAC. The generated 4-level signal is loaded into AWG at sampling rate of 120-GSa/s and modulated on the 1550 nm optical carrier with a Mach-Zehnder modulator (MZM). The optical signal is launched into a G.652 fiber link at the power of 5.5 dBm. After 40-km or 50-km SSMF transmission, the ROP into the receiver is controlled by a variable optical attenuator (VOA). Then the optical signal is boosted with an Erbium-doped fiber amplifier (EDFA) and directly detected by a single-end photodiode (PD). The received electrical signal is sampled by an oscilloscope (Keysight DSAV334A) at 80-GSa/s sample rate. To block out the residual high-frequency noise, we limit the bandwidth of oscilloscope to 25 GHz. The received signal is processed offline, and the DSP includes clock data recovery (CDR), match filter, THP decoding, PAM de-mapping and BER counter. THP decoding includes an equalizer and modulo operation. We apply 2-order PNLE with taps ($N_1 = 51,\ N_2 = 15$) to decode the signal. The total number of taps for PNLE is only 66. The PNLE requires 81 multipliers per symbol. The performance of the IM/DD system is evaluated with pre-FEC BER.

IV. Results

The performance of the proposed 2-bit cost-effective THP transmitter scheme in a 40-km SSMF PAM-4 IM/DD transmission is evaluated and compared with a common scheme using DFE in the receiver DSP. The DFE contains 51 feedforward taps and 9 feedback taps. The signals transmitted in both schemes are quantized to 2 bits and noise shaped.

Fig. 8 shows the BER versus ROP curves of the schemes using THP/DFE and different up-sampling rate. Comparing DFE and THP schemes, only the BER performance of the THP scheme achieves 1.35×10^{-2} after 40-km transmission at ROP of -4-dBm, which is below the OFEC threshold 2×10^{-2}. Theoretically, both THP and DFE have equivalent transfer functions and same anti-dispersion abilities. Nevertheless, due to the influence of error propagation, the BER of the DFE scheme is markedly higher than that of the THP scheme due to error propagation. When comparing the impact of up-sampling rates on BER, a higher up-sampling rate can expel more quantization noise from the signal band and improve performance. When the up-sampling rate increases from 80 GSa/s to 120 GSa/s, there is an improvement in the BER performance from 6.50×10^{-2} to 1.35×10^{-2}.

In Fig. 9(a), we evaluate the impact of the physical number of bits (PNOB) of DAC on the BER performance at ROP of -4 dBm. The use of a low-resolution DAC without noise shaping significantly reduces the performance, even though up-sampling has already diluted the in-band noise. 2-bit quantization increases the BER to 8.22×10^{-2}. Applying noise shaping brings the BER performance of our scheme close to the 4-bit and 8-bit DAC case at ROP of -4 dBm. Fig. 9(b) reveals that the overall performance of our scheme is close to the case using an 8-bit DAC. It slightly underperforms only when the ROP is higher than -6 dBm. The BER gap is only about 2×10^{-3}.

As is discussed in Section III, we use probabilistic shaping PAM modulation to reduce modulo loss and further extend the

distance in the transmission experiment. In the 50-km transmission, the THP includes 11 feedback taps. And a PNLE with taps ($N_1 = 51$, $N_2 = 21$) is utilized to decode the signal. A symmetric probability distribution of the four levels is adopted as $[p,\ 0.5-p,\ 0.5-p,\ p]$. Fig. 10(a) shows the BER versus the probability p curve of the 50-km PS-PAM-4 transmission. The corresponding bit-per-symbol rate is also attached in the figure. Reducing the probability p improves the BER performance of the system. Trading off the rate and BER, as illustrated in Fig. 10(b), with 1.88-bit/symbol PS-PAM-4 modulation ($p = 0.15$), the proposed scheme achieves a BER of 1.57×10^{-2} at ROP of -6-dBm after 50-km transmission.

V. Conclusion

In this paper, a cost-effective C-band IM/DD transmission scheme is proposed for ER inter-DCI utilizing only 2-bit DAC. THP is used to pre-compensate the dispersion-induced impairments. In order to generate the encoded signal with a low-resolution DAC, upsampling and quantization noise shaping is used to improve the SNR. We experimentally demonstrate a C-band 40-Gbaud DSB PAM-4 for 40-km and PS-PAM-4 for 50-km SSMF transmission without any optical dispersion compensation. The ROP performance of the proposed scheme using a 2-bit DAC is proximate to the common case of using an 8-bit DAC. The BER performance achieves 1.57×10^{-2} after 50-km SSMF transmission at ROP of -6-dBm, which is below the 15.3% OFEC threshold.

References

[1] C. Kachris and I. Tomkos, "A survey on optical interconnects for data centers," *IEEE Commun. Surveys Tuts.*, vol. 14, no. 4, pp. 1021–1036, Fourth Quarter 2012, doi: 10.1109/SURV.2011.122111.00069.

[2] H. Xin et al., "Nonlinear Tomlinson-Harashima precoding for direct-detected double sideband PAM-4 transmission without dispersion compensation," *Opt. Exp.*, vol. 27, no. 14, pp. 19156–19167, 2019, doi: 10.1364/OE.27.019156.

[3] J. Li, Z. Wang, X. Li, and Y. Su, "Single-span IM/DD transmission over 120-km SMF with a silicon photonic Mach-Zehnder modulator and THP," in *Proc. Opt. Fiber Commun. Conf.*, 2022, Paper M2H.3, doi: 10.1364/OFC.2022.M2H.3.

[4] Y. Yoffe et al., "Low-resolution digital pre-compensation enabled by digital resolution enhancer," *J. Lightw. Technol.*, vol. 37, no. 6, pp. 1543–1551, Mar. 2019, doi: 10.1109/JLT.2018.2885452.

[5] M. Yin, X. Wang, D. Zou, W. Wang, Q. Sui, and F. Li, "Low cost O-band inter-datacenter interconnect utilizing a 4-bit resolution digital-to-analog converter for PAM-4 signal generation," *Opt. Exp.*, vol. 29, no. 20, pp. 31527–31536, 2021, doi: 10.1364/OE.431344.

[6] M. Yin, D. Zou, W. Wang, F. Li, and Z. Li, "Transmission of a 56 Gbit/s PAM4 signal with low-resolution DAC and pre-equalization only over 80 km fiber in C-band IM/DD systems for optical interconnects," *Opt. Lett.*, vol. 46, pp. 5615–5618, 2021, doi: 10.1364/OL.441598.

[7] L. Shu, Z. Yu, K. Sun, H. Huang, Z. Wan, and K. Xu, "Performance investigation of error-feedback noise shaping in low-resolution high-speed IM/DD and coherent transmission systems," *J. Lightw. Technol.*, vol. 40, no. 12, pp. 3669–3680, Jun. 2022, doi: 10.1109/JLT.2022.3153387.

[8] J. Kim et al., "A 224-Gb/s DAC-based PAM-4 quarter-rate transmitter with 8-tap FFE in 10-nm FinFET," *IEEE J. Solid-State Circuits*, vol. 57, no. 1, pp. 6–20, Jan. 2022, doi: 10.1109/JSSC.2021.3108969.

[9] S. Kiran et al., "A 56GHz receiver analog front end for 224 Gb/s PAM-4 SerDes in 10 nm CMOS," in *Proc. Symp. Very Large Scale Integration Circuits*, 2021, Paper C21-1, doi: 10.23919/VLSICircuits52068.2021.9492471.

[10] Q. Hu et al., "120 GSa/s BiCMOS AMUX for 360 Gbit/s high-information-rate signal generation demonstrated in 10 km IM/DD system," *J. Lightw. Technol.*, vol. 40, no. 5, pp. 1330–1338, Mar. 2022, doi: 10.1109/JLT.2021.3133409.

[11] R. Hersent et al., "Analog-multiplexer (AMUX) circuit realized in InP DHBT technology for high order electrical modulation formats (PAM-4, PAM-8)," in *Proc. 23rd Int. Microw. Radar Conf.*, 2020, pp. 222–224, doi: 10.23919/MIKON48703.2020.9253772.

[12] F. Li, Z. Luo, M. Yin, X. Wang, and Z. Li, "Architectures and key DSP techniques of next generation passive optical network (PON)," in *Proc. Opt. Fiber Commun. Conf. Exhib.*, 2022, Paper M3G.4, doi: 10.1364/OFC.2022.M3G.4.

[13] M. Yin et al., "Pre-equalized DMT signal transmission utilizing low-resolution DAC with channel response dependent noise shaping technique," *J. Lightw. Technol.*, vol. 41, no. 10, pp. 3065–3073, May 2023, doi: 10.1109/JLT.2023.3235721.

[14] H. Harashima and H. Miyakawa, "Matched-transmission technique for channels with intersymbol interference," *IEEE Trans. Commun.*, vol. 20, no. 4, pp. 774–780, Aug. 1972, doi: 10.1109/TCOM.1972.1091221.

[15] W. Yu, D. P. Varodayan, and J. M. Cioffi, "Trellis and convolutional precoding for transmitter-based interference presubtraction," *IEEE Trans. Commun.*, vol. 53, no. 7, pp. 1220–1230, Jul. 2005, doi: 10.1109/TCOMM.2005.851605.

[16] W. A. Ling, "Shaping quantization noise and clipping distortion in direct-detection discrete multitone," *J. Lightw. Technol.*, vol. 32, no. 9, pp. 1750–1758, May 2014, doi: 10.1109/JLT.2014.2304242.

[17] P. Schulte and G. Böcherer, "Constant composition distribution matching," *IEEE Trans. Inf. Theory*, vol. 62, no. 1, pp. 430–434, Jan. 2016, doi: 10.1109/TIT.2015.2499181.